Iranian J Biotech. October 2020;18(4): e2553 DOI: 10.30498/IJB.2020.2553

Research Article

Structural Studies on an Anti-Angiogenic Peptide Using Molecular Modeling

Elham Assareh[1], Faramarz Mehrnejad[2], S. Mohsen Asghari*[1,3]

[1] Department of Biology, Faculty of Sciences, University of Guilan, Rasht, Iran
[2] Department of Life Sciences Engineering, Faculty of New Sciences & Technology, University of Tehran, Tehran, Iran
[3] Institute of Biochemistry and Biophysics (IBB), University of Tehran, Tehran, Iran

*Corresponding author: Mohsen Asghari, Department of Biology, Faculty of Sciences, University of Guilan, P.O. BOX: 41335-19141, Rasht, Iran, Tel /Fax: +98 1333333647, E-mail: sm_asghari@guilan.ac.ir

Background: Development of VEGF antagonists, which inhibit its interaction with the receptors, is a widely used strategy for the inhibition of angiogenesis and tumor growth.
Objectives: In the present study, a VEGFR-1 antagonistic peptide was designed and its potential for binding to VEGFR-1 and VEGFR-2 was evaluated by theoretical studies.
Materials and Methods: Based on the X-ray structure of VEGF-B/VEGFR-1 D2 (PDB ID: 2XAC), an antagonistic peptide (known as VGB1) was designed, and its model structure was constructed using homology modeling in the MODELLER, version 9.16. The validity of the modeled structures was estimated employing several web tools. Finally, one model was chosen and molecular dynamics (MD) simulation was applied using the GROMACS package, version 5.1.4, to allow conformational relaxation of the structure. Next, docking process of the peptide with VEGFR-1 and VEGFR-2 was performed by HADDOCK web server and the docking structures were optimized by MD simulation for 20 ns. The far-UV circular dichroism (CD) spectrum of VGB1 was recorded to evaluate the overall structure of the peptide.
Results: The far-UV CD spectrum indicated that VGB1 contains α helix structure. The results from docking studies suggested that Van der Waals and nonpolar interactions play the most important role in the peptide binding to VEGFR-1. In addition, our results implicated the relevance of both Van der Waals and electrostatic interactions in the formation of complex between VGB1 and VEGFR-2. In addition to the common binding residues in the corresponding region of VEGF-A and VEGF-B, additional binding residues also were predicted for the interaction of VGB1 with VEGFR-1 and VEGFR-2.
Conclusions: The results of MD and molecular docking simulations predicted that VGB1 recognizes both VEGFR-1 and VEGFR-2, which may lead to the prevention of the downstream signaling triggered by these receptors.

Keywords: Antagonistic peptide; Docking; MD simulation; VEGFR

1. Background

Angiogenesis is the formation of new blood vessels from pre-existing ones. Furthermore, it is involved in the development of tumors from a benign to a malignant state. As a result of angiogenesis, tumor cells can penetrate into blood or lymphatic vessels, circulate through the intravascular stream, and then proliferate at another site, which is known as metastasis (1). Vascular endothelial growth factor (VEGF) family are known as the most important angiogenic proteins, comprising a cysteine-knot motif that made up of three intertwined disulfide bridges. Disulfide bridges exist in both intra- and inter-chain forms and create an individual functional sign that is supposed to be major determinants of protein stability and folding. These cysteine residues connectivity stabilize the Cα skeleton of these polypeptides for the amplification of the solvent-exposed loop regions and forms the ligand-binding surface on these receptors. (2). VEGFs family comprise VEGF-ligands and -receptors (VEGFRs). The VEGF ligand-receptor system triggers and regulates angiogenic and/or lymphangiogenic pathways. VEGF ligands are inclusive VEGF-A, VEGF-B, VEGF-C, VEGF-D, VEGF-E, VEGF-F, and PLGF; VEGFRs contains three members: VEGFR-1, VEGFR-2, and VEGFR-3. As a result of alternative splicing, four subtypes of VEGF-A are produced; VEGF-A 121, 165, 189 and 206 (3) among which VEGF-A 165 is the most important of the subtype which triggers the development and maintenance of blood vessel network through binding to VEGFR-2. VEGF-A increases angiogenesis, vascular permeability, cell migration, and

proliferation through interaction to both VEGFR-1 and VEGFR-2 (4, 5). The signaling cascade triggered by the VEGF-A/VEGFR-2 system also is essential for cancer cell proliferation and survival (5).

First evidence connecting VEGFR-1 to endothelial cell function and angiogenesis, was given by targeted deletion of VEGFR-1, that resulted in early embryonic lethality due to irregular blood vessel growth (6). VEGF-B affects blood vessel formation by binding to VEGFR-1. This factor exists as two isoforms, VEGF-B 167 and VEGF-B 186, arising from distinctive spliced mRNA and binds specifically to VEGFR-1 (7-9). There is growing data on the critical role performed by VEGF-B in angiogenesis. VEGF-B also has been involved in several pathological conditions such as tumor growth and metastasis (10).

VEGF-A and VEGF-B have high sequence homology and bind to the VEGFR-1 D2 domain in the same way. The binding sites of these ligands to the VEGFR are an α1 helix, loop 2, and loop 3. The hydrophobic interactions have chief role in binding of the α1 helix with VEGFR-1 D2. The sequence alignment of VEGF-A and VEGF-B revealed they have a considerable identity in N-terminal α1 helix area (11-13). Therefore, a peptide mimicking the N-terminal α1 helix of VEGF-B, probably can compete with both VEGF-B and VEGF-A in binding to VEGFR-1 or VEGFR-2 and would be useful for the cancer treatment.

2. Objectives

In the present study, we designed a 17-amino acid peptide (referred to as VGB1) based on the crystal structure of VEGF-B/R1 D2 complex (PDB ID: 2XAC). The secondary structure of the peptide was evaluated by molecular modeling and CD spectroscopy. The interactions of the peptide with VEGFR-1 and VEGFR-2 were evaluated and compared with those of VEGF-B and VEGF-A.

3. Materials and Methods

3.1. Building Model

A model of the designed peptide was constructed using homology modeling in the MODELLER software, version 9.16 (14). The sequence of VEGF-B (PDB ID: 2C7W) was considered as a template. The homology modeling consists of the following steps: (i) template selection; (ii) alignment between the target sequence and the template sequence; (iii) model building, and (iv) model evaluation. The template selection was performed by BLAST web server (http://blast.ncbi.nlm.nih.gov/Blast/). The sequence identity of the template (VEGF-B, PDB ID: 2C7W) with the peptide was defined to be 75%. The fasta format of VEGF-B was obtained from the PDB website (http://www.rcsb.org/pdb/). Sequence alignment was performed using the multiple sequence alignment online server ClustalW (https://embnet.vital-it.ch/software/ClustalW.html). Ten models were generated by MODELLER software, version 9.16, and the quality of the modeled structures was evaluated utilizing full model analysis via the SWISS-MODEL web server (http://swissmodel.expasy.org/). Finally, the best model was selected and considered for further analyses.

3.2. Structural Refinement

Structural refinement was performed using GROMACS package, version 5.1.4 (15). The 54A7 force-field (16) parameters were used for simulation. The interaction time-steps were set to 2 fs during the whole simulation time. The long range electrostatic interactions were calculated utilizing the Particle-Mesh Ewald (PME) method with an interpolation order of 4 and maximum Fast Fourier Transforms (FFT) grid spacing of 0.16 nm. A cut-off radius of 1.0 nm was applied for Coulomb interactions and the short range interactions defined as van der Waals, was set to a cut-off of 1.0 nm (17). Periodic boundary conditions were utilized and the bonds were restrained using the LINCS algorithm to their equilibrium position. To fully cover the protein system in water, initial structure was solvated with three-point model water molecules in a cubic box of 1.0 nm following periodic boundary conditions (PBC). The created system was then neutralized through "genion tool" plugin of GROMACS package by adding Na and Cl ions. The system was minimized for 50000 iterations using the steepest descent (SD) algorithm. The studied system was simulated under isothermal-isobaric ensemble (NPT) for 5 ns at constant temperature and pressure of 300 K and 1 atm respectively, using velocity rescaling (modified Berendsen) temperature coupling and Parrinello-Rahman pressure coupling methods. The equilibration (NVT and NPT) was performed for 50000 steps. After implementation of minimization and equilibration procedures, one system of the peptide was subjected to 175 ns production run of MD simulations utilizing 2 fs as the time step. Coordinates of all atoms were recorded in the form of .trr GROMACS trajectory file for every 10 ps. Checking of model quality for final trajectory was conducted utilizing TM-align web tool (18) to enhance the accuracy of validation.

3.3. Molecular Docking and MD Simulation of Docking Clusters

The HADDOCK protocol (19) was used to dock VGB1 to VEGFR-1 as well as VEGFR-2. The docking process in HADDOCK is driven by identified obscure interaction restraints about the binding interface. Thus, residues that have previously been resolved to be involved in VEGF-B/VEGFR-1 D2 binding interface were designated as active residues. Based on the crystal structure of VEGF-B/VEGFR-1 D2 complex (PDB ID: 2XAC), the interface surface residues in VEGFR-1 (Pro143, Phe172, Leu204, Leu221) together with interface residues of VEGF-B (that are corresponding to Trp3, Ile4, Tyr7, Thr8, Thr11, Cys12, Gln13 of VGB1) were utilized as active residues, and neighboring residues of active residues were utilized as passive residues.

On the based on the crystal structures of VEGF-A/VEGFR-2 (PDB ID: 3V2A) and VEGF-A/VEGFR-1 D2 (PDB ID: 1FLT), three amino acids that play a critical role in binding to VEGFR-2, as well as VEGFR-1, were considered as docking criterion of the peptide to VEGFR-2. Based on the sequence alignment of VEGF-A and VEGF-B (12), corresponding residues with these three amino acids of VEGF-B are accessible on the same receptor-binding face as the KDR-binding determinants in VEGF-A. These include residues 17, 21, and 25 (that are corresponding to the residues Trp3, Tyr7, and Thr11 of VGB1) and together with interface residues in VEGFR-2 (Tyr165, Met197, and I215) were defined as active residues, and neighboring residues of active residues were defined as passive residues. In the next step, the molecular docking structures were simulated by MD simulation for 20 ns (as described in Section *3.2.*). The goal of this step was to optimize the interactions and binding energies in the clusters.

3.4. Peptide Synthesis

The peptide was synthesized by Shine Gene Biotechnologies, Inc., Shanghai, China. The purity of the peptide was determined ~ 95% by high-performance liquid chromatography (HPLC), examined by matrix-assisted laser desorption/ionization time-of-flight mass spectrometry (MALDI-TOF), and established by electrospray ionization mass spectrometry (ESI-MS) analysis. The Ellman assay (20, 21) was utilized to confirm the presence of the disulfide bond in the peptide (data not shown).

3.5. Far-UV CD Measurement

Far-UV CD spectra were recorded by a Circular Dichroism Spectrometer (Aviv Model-215) at 25 °C. The peptide was dissolved in Tris, 20 mM; pH 7.5 and the final concentration was 0.5 $mg.mL^{-1}$. An average of three scans was recorded from 190 to 250 nm, and the buffer spectrum was subtracted from their corresponding sample spectrum using the software provided by the manufacturer. The cuvette path length was 0.1 cm. The secondary structure was estimated using CDNN software provided by the manufacturer.

4. Results

4.1. Peptide Design

Two complexes VEGF-B/VEGFR-1 D2 (PDB ID: 2XAC) and VEGF-A/VEGFR-1 D2 (PDB ID: 1FLT) have three binding sites on dimeric ligands; N-terminal α1 helix (residues 17-25), loop 2 (loop 61-67) and loop 3 (loop 84-89). Data from sequence alignment of VEGF-A and VEGF-B indicates these two ligands have a high identity in N-terminal α1 helix region and residues participating in the receptor-binding interface (12). Therefore, it is feasible that an antagonist mimicking the N-terminal α1 helix of VEGF-B, could compete with both VEGF-A and VEGF-B and targets both VEGFR-1 and VEGFR-2, interfering with their signaling pathways and dependent angiogenesis. In this study, a 17-mer α1 helix mimicking peptide (known as VGB1) with sequence $_2$HN-CSWIDVYTRATCQPRPL-COOH was designed based on the crystal structure of VEGF-B/VEGFR-1 D2. The results of several studies showed cyclic peptides had better helical conformation and increased affinity for their receptor compared to the corresponding linear peptides (22-24). Here, a non-ended disulfide bond was created between Cys1 and Cys12 so that a peptide with motif RPL in C-terminal was obtained.

4.2. Molecular Modeling, Structural Refinement and Evaluation of Three-Dimensional (3D) Structure of VGB1

A 3D model of the peptide was made using the MODELLER software, version 9.16. One out of 10 models was chosen, and the quality of the predicted 3D model was validated using full model analysis by means of the SWISS-MODEL web server (http://swissmodel.expasy.org/). Ramachandran plot analysis illustrated that 100% of residues were located in the favored regions. There was no residue in the disallowed region of Ramachandran plot (**Fig. 1A**). The overall model quality was estimated by QMEAN Z-score and was determined -0.96 that implicates good quality of the model compared to the non-redundant set of PDB structures (**Fig. 1B**) (25). The confirmed model of

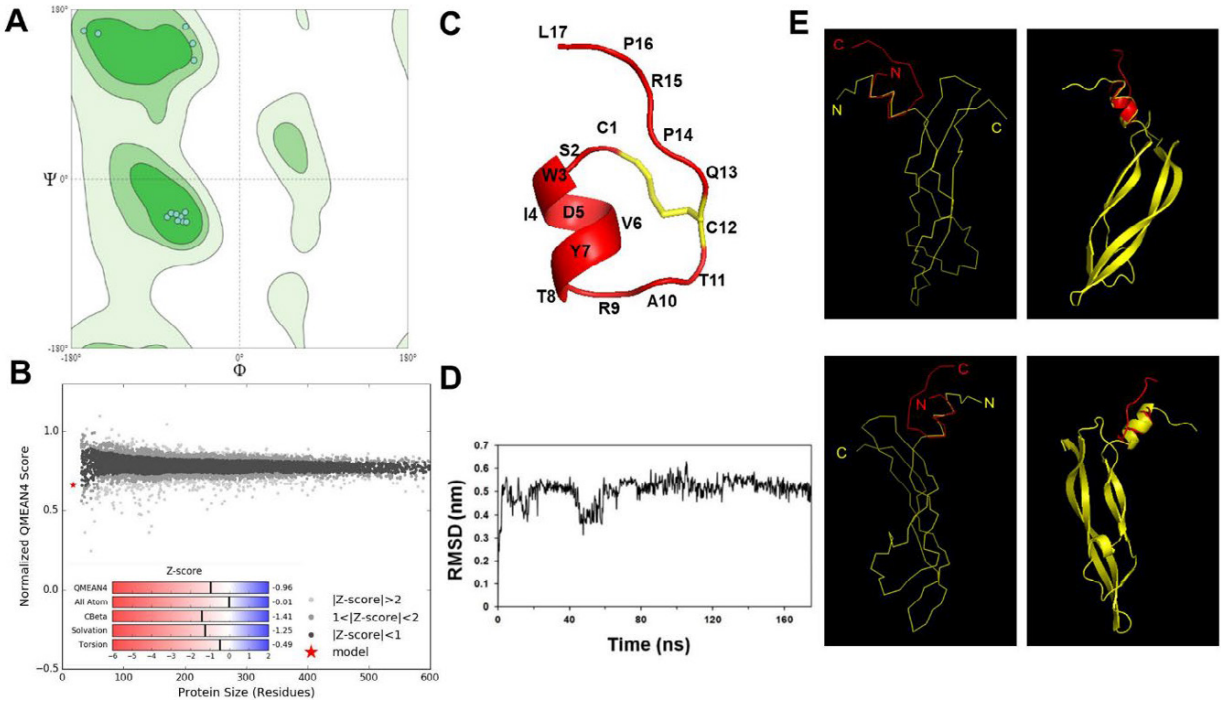

Figure 1. Validation of VGB1 model by SWISS-MODEL web server. (A) Ramachandran plot. The plot is shown that 100% of residues were located in the favored regions. (B) QMEAN Z-score plot of modeled 3D structure of VGB1. (C) Three-dimensional model of VGB1. (D) RMSD analysis. (E) Structural alignment of VGB1 (red) with VEGF-B (yellow; up) and VEGF-A (yellow; bottom).

VGB1 was subjected to energy minimization by MD simulation (**Fig. 1C**). Root-mean-square deviation (RMSD) represents the mean of Cα changes during simulation time and is an appropriate criterion for the evaluation of protein or peptide stability during MD simulation. The trajectory of 175 ns simulation showed acceptable stability and no significant deviation after 80 ns (**Fig. 1D**). Dictionary of the secondary structure of proteins (DSSP) defines the secondary structure of peptides or proteins gave a set of 3D coordinates. DSSP analysis for the peptide proposed the presence of α helix in VGB1 (**Table 1**). The 3D model of VGB1 was compared with the template structure (PDB ID: 2C7W) by a structural alignment using TM-align web tool. TM-score of VGB1 structural alignment was computed to be 0.1. TM-score increased to be 0.74 when the corresponding region with VGB1 of VEGF-B contains α1 helix was considered as a template, implicating a high accuracy of constructed model by homology modeling method (two structures with 0.5 < TM-score < 1 have almost the same fold) (**Fig. 1E**). Also, the 3D model of VGB1 was compared with the N-terminal α1 helix of VEGF-A and resulting in a TM-score to be 0.63.

4.3. Analysis of Complex Structures of VGB1 with VEGFR-1 and VEGFR-2

Molecular docking simulations were performed to investigate the interaction of VGB1 with both VEGFR-1 and VEGFR-2. The residues involved in the interaction of VEGF-B with VEGFR-1 D2 (13), including Trp3, Ile4, Tyr7, Thr8, Thr11, Cys12 and Gln13 (corresponding to Trp17, Ile18, Tyr21, Thr22, Thr25, Cys26 and Gln26 in VEGF-B), were considered as active residues for docking of VGB1 to VEGFR-1 D2. It has been shown residues Phe17, Tyr21 and Tyr25 are the key residues for the interaction of VEGF-A with VEGFR-2 (12). Therefore, residues Trp3, Tyr7, and

Table 1. The percentage of secondary structure obtained by DSSP analysis

Secondary structure (%)				
α Helix	**β Bridge**	**Turn**	**coil**	**Bend**
35.3	1.5	18	35	10.2

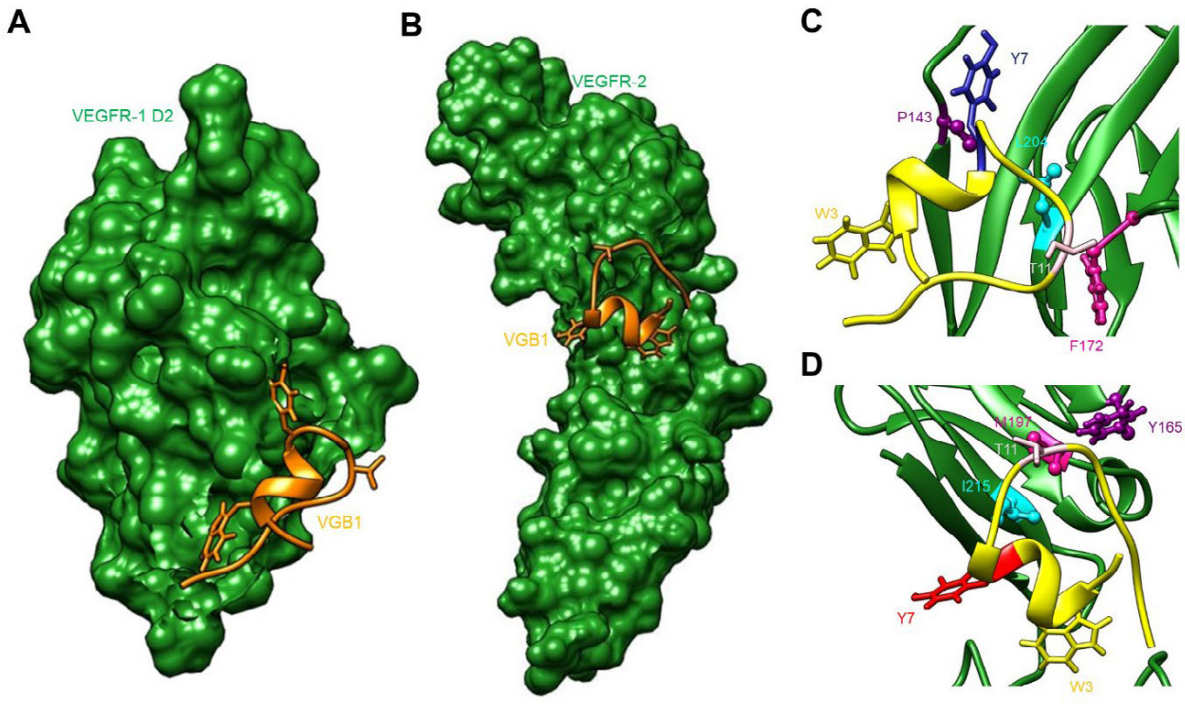

Figure 2. VGB1 in complex with VEGFR-1 and -2. (A) VGB1/VEGFR-1 and (B) VGB1/VEGFR-2 complexes obtained by molecular docking simulation. Some residues participating in hydrophobic interactions in (C) VGB1/VEGFR-1 and (D) VGB1/VEGFR-2. These residues also contribute to hydrophobic interactions in VEGF-B/VEGFR-1, VEGF-A/VEGFR-1, and VEGF-A/VEGFR-2 complex.

Table 2. A comparison of hydrophobic interactions in the VEGF-B/VEGFR-1, VEGF-A/VEGFR-1, and VGB1/VEGFR-1

Hydrophobic interactions					
Receptor			Ligand		
VEGF-B/VEGFR-1 Complex	VEGF-A/VEGFR-1 Complex	VGB1/VEGFR-1 Complex	VEGF-B/VEGFR-1 Complex	VEGF-A/VEGFR-1 Complex	VGB1/VEGFR-1 Complex
Pro143 Phe172 Leu204 Leu221	Ile142 Pro143 Thr166 Phe172 Pro173 Leu204	Glu141 Ile142 Pro143 Ile145 His147 Phe172 Pro173 Ile202 Gly203 Leu204 Thr222 His223	#Trp17 $Ile18 *Tyr21 &Thr22 ¤Thr25 Cys26 Gln27	#Phe17 $Met18 *Tyr21 &Gln22 ¤Tyr25	#Trp3 $Ile4 Val6 *Tyr7 Ala10 ¤Thr11 Gln13 Pro14 Pro16 Leu17

#, $, *, &, ¤ These symbols show corresponding residues in VEGF-B, VEGF-A and VGB1.

Thr11 were also considered as a criterion for docking of VGB1 to VEGFR-2. The most stable clusters which had the most negative HADDOCK score and Z- score were simulated for 20 ns to optimize the interactions in the docking clusters (**Fig. 2A** and **2B**).

According to the complex structures between VEGF-B with VEGFR-1 and between VEGF-A with VEGFR-1 and -2, residues at positions 17, 21 and 25 (Trp17, Tyr21, and Thr25 in VEGF-B; and Phe17, Tyr21 and Phe25 in VEGF-A) are critical for the interaction

Table 3. A comparison of hydrophobic interactions in the VEGF-A/VEGFR-2 and VGB1/VEGFR-2

Receptor		Ligand	
VEGF-A/VEGFR-2 Complex	**VGB1/VEGFR-2 Complex**	**VEGF-A/VEGFR-2 Complex**	**VGB1/VEGFR-2 Complex**
Tyr165	His133	#Phe17	Cys1
Met197	Val135	$Met18	Ser2
Ile215	Arg164	*Tyr21	#Trp3
	Tyr165	&Gln22	$Ile4
	Gly196	¤Tyr25	Asp5
	Met197		Val6
	Met213		*Tyr7
	Ile215		Ala10
	Val254		¤Thr11
	Gly255		Pro14
	Asp257		Arg15
	Glu284		Leu17
	Lys286		
	Ser311		
	Gly312		

#, $, *, &, ¤ These symbols show corresponding residues in VEGF-A and VGB1.

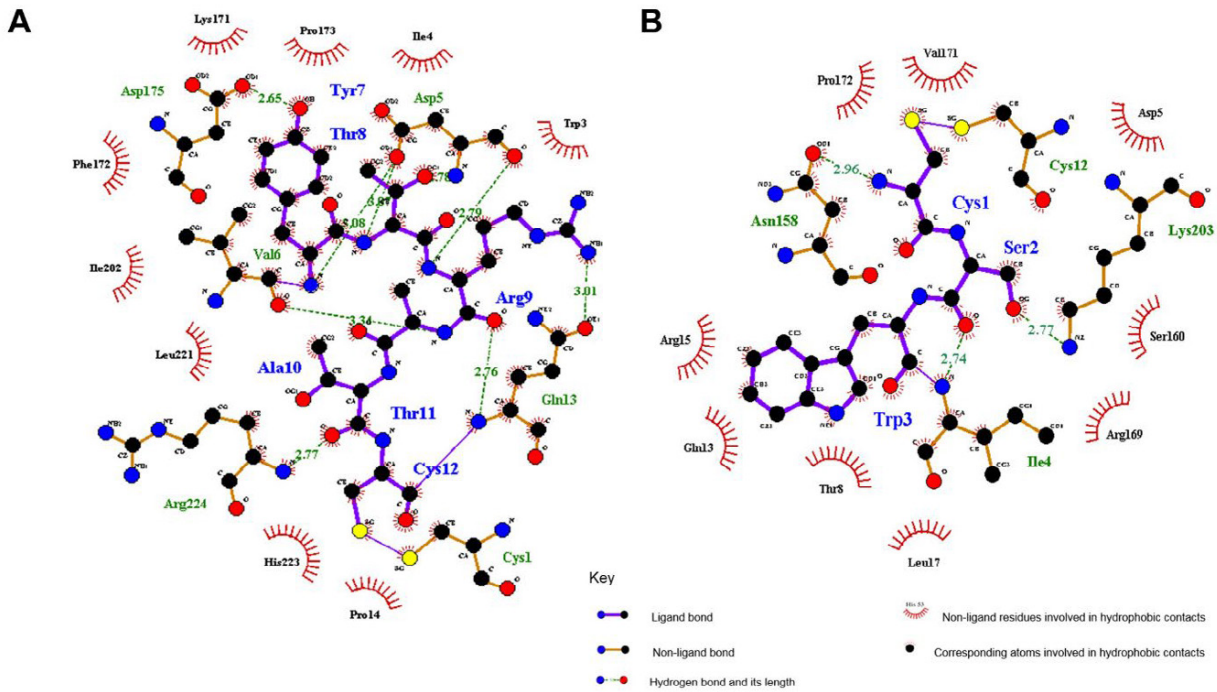

Figure 3. Two-dimensional representation of H-bonds in the VGB1/VEGFR-1 D2 and VGB1/VEGFR-2 complex. (A) Representation of H-bonds in the VGB1/VEGFR-1 D2 complex. There are two inter-chain and six intra-chain H-bonds among the interactions between VGB1 and VEGFR-1 D2. (B) Representation of H-bonds in the VGB1/VEGFR-2 D2 complex. There are two inter-chain and one intra-chain H-bonds in the VGB1/VEGFR-1 D2 complex.

between ligands and the receptors. Importantly, based on the binding energy analysis by MMPBSA method (26), equivalent residues (Trp3, Tyr7, and Thr11) are key residues for the binding of VGB1 to VEGFR-1 and -2 (**Fig. 2C** and **2D**). Furthermore, apparently, a large number of residues participate in the formation of VGB1/receptor complex compared to VEGF-A or -B/receptor complex (**Table 2** and **Table 3**).

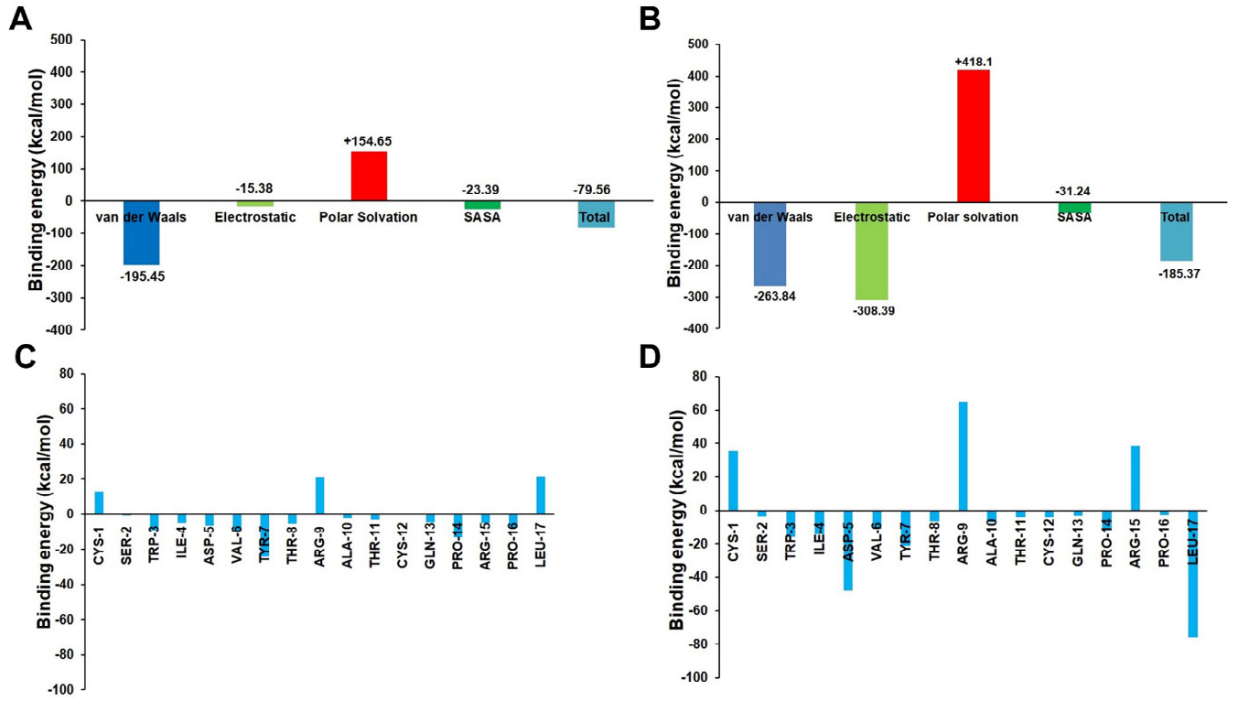

Figure 4. Binding energy analysis. The binding energy plot of (A) VGB1/VEGFR-1 and (B) VGB1/VEGFR-2 complex. The total binding energy of VGB1/VEGFR-2 complex is more negative than it to VGB1/VEGFR-1 complex that suggests VGB1/VEGFR-2 complex is more stable than VGB1/VEGFR-1 complex. Total binding energies for residues of VGB1 in (C) VGB1/VEGFR-1 and (D) VGB1/VEGFR-2 complex.

Table 4. Far-UV circular dichroism spectroscopy analysis

Secondary structure (%)			
α Helix	**β sheet**	**β turn**	**random coil**
32	8	22	38

There are two H-bonds among the interactions between the peptide and the VEGFR-1 D2; The first between the amino acids Tyr7 and Asp175 (bond length: 2.65 A°) and the second between the amino acids Thr11 and Arg224 (bond length: 2.77 A°) (**Fig. 3A**). The H-bonds observed in the VEGF-B/VEGFR-1 D2 complex are generated between ligand amino acids, but not between the ligand and receptor amino acids. Also, there are two H-bonds in the VGB1/VEGFR-2 complex; one between the amino acids Cys1 and Asn158 (bond length: 2.96 A°) and other between the amino acids Ser2 and Lys203 (bond length: 2.77 A°) (**Fig. 3B**). Similar to the binding of VEGF-B to VEGFR-1, as well as, VEGF-A to VEGFR-1 and -2, hydrophobic interactions play an important role in VGB1 binding to these receptors (**Fig. 4A** and **4B**). The residues Trp3, Tyr7, and Thr11 (corresponding to Trp17, Tyr21, and Thr25 in VEGF-B) participate in these interactions (**Fig. 4C** and **4D**). Although, electrostatic interactions also have a considerable role in binding of the peptide with VEGFR-2 (**Fig. 4B**).

4.4. Far-UV Circular Dichroism Spectroscopy

The CD spectroscopy was executed to determine whether the peptide had a secondary structure. Estimation of the content of secondary structure indicated the possibility of the presence of secondary structure α helix in VGB1 (**Table 4**).

5. Discussion

Although many peptides have been designed based on VEGF-A/VEGFRs complex, so far few studies were conducted for the peptide design based on VEGF-B/VEGFR-1 D2 complex structure (23). In the case of peptides derived from VEGF-B, previous studies focused on the interaction with VEGFR-1. Given that disability of VEGF-B in binding to VEGFR-2, so far, the ability of one peptide mimicking VEGF-B was not investigated for interaction with this receptor. Designing of a peptide based on a region of VEGF-B with a

significant identity with VEGF-A sequence antagonizing VEGF-B/VEGFR-1 complex that also capable for binding to VEGFR-2 and disrupt VEGF-A/VEGFR-2 signaling will applicable for angiogenesis inhibition and treatment of the immoderate angiogenesis-dependent disorders. In the present study, an antagonistic peptide was designed based on the available crystal structure of VEGF-B/VEGFR-1 D2 complex (PDB ID: 2XAC). The modeling of the peptide and the subsequent structure relaxation of the model suggested an α helix secondary structure. Docking studies were conducted to determine whether this peptide was able to bind to both receptors VEGFR-1 and VEGFR-2.

It has been noted that the presence of the helical structure in peptides mimicking the N-terminal α1 helix of VEGF-A and -B plays an important role in the binding of these peptides to their receptors (27). The far-UV CD spectra denoted that VGB1 contains α helix structure. The content of α helix structure (32%) proposed that about 5 to 17 residues in VGB1 follows the helical structure. In agreement with this data, DSSP analysis of the peptide proposed that 6 out of 17 residues, including fragment Trp3 to Thr8 (corresponding to residues Trp17 to Thr22 in VEGF-B) of VGB1, follows the helical structure (**Table 1**). The model quality evaluation by TM-align web tool also suggested that VGB1 is a good mimic from N-terminal α1 helix structure of both VEGF-B and VEGF-A (TM-score 0.74 and 0.63, respectively). The residues Trp17, Ile18, Tyr21, Thr22 and Thr25 in N-terminal α1 helix of VEGF-B are notably similar to KDR-binding residues in α1 helix of VEGF-A (Phe17, Met18, Tyr21, Gln22, and Tyr25) (12, 13). On the other hand, it was found that aromatic residues Trp17 and Tyr21 in VEGF-B and Phe17, Tyr21 and Tyr25 in VEGF-A engage in the interaction with the receptors. Our theoretical analysis suggested aromatic binding residues Trp3 and Tyr7 (corresponding to the residues Trp17 and Tyr21 in VEGF-B) placed in the α helix. The presence of the disulfide bond and the formation of cyclic structure in VGB1 may contribute to the preservation of the α helix conformation and its potential to interact with the receptor.

The energy analysis data proposed VGB1, similar to the corresponding region of VEGF-B, binds to VEGFR-1 mainly by hydrophobic interactions (**Fig. 4A**). The sequence CPQPRPLC was determined to binding with VEGFR-1 and neuropilin-1 (NRP-1) but not with VEGFR-2 (28-30). Therefore, it will be probable that the sequence CQPRPL at C-terminal contributes to the ability of VGB1 for binding to VEGFR-1. This hypothesis was strengthened by investigating the critical residues in the formation of hydrophobic interactions in VGB1/VEGFR-1 complex (**Table 2**). The binding energy analysis suggested that the peptide has a greater number of interactions than the corresponding region in the monomeric VEGF-B. Two reasons can be mentioned for these excessive interactions: first, VGB1 is smaller than VEGF-B, resulting in fewer spatial inhibition by the surrounding side chains and more effectively ligate with VEGFR-1; second, interactions in the crystal structure, which is a water-free environment, are different from the intracellular aquatic environment. Of note, the simulation of peptide-receptor complex was performed in a box filled with water and is similar to the intracellular environment. The results of molecular docking study indicating that VGB1 can bind to VEGFR-2 in addition to VEGFR-1. Surprisingly, a comparison of the total binding energy between the VGB1/VEGFR-1 D2 and the VGB1/VEGFR-2 complexes suggests that VGB1 even likely created a more stable complex with VEGFR-2 than VEGFR-1 D2 (**Fig. 4B**). The molecular docking simulation reveals that both hydrophobic and electrostatic interactions are important in the formation of the VGB1/VEGFR-2 complex (**Fig. 4B**). Also, among the seven important amino acids in the formation of this complex, three amino acids were corresponding with the critical amino acids in the binding interface of the VEGF-A/VEGFR-2 complex (residues 17, 21, and 25) (**Table 3** and **Fig. 4D**). Given that the sequence CPQPRPLC does not bind to VEGFR-2 (28-30), it seems to be improbable that fragment CQPRPL participates in the binding of VGB1 to VEGFR-2. In contrary with this hypothesis, the results from binding energy analysis suggest that segment CQPRPL also probably is important in the property of VGB1 for interaction with VEGFR-2 (**Fig. 4D**).

6. Conclusions

In this study, we designed a peptide mimicking N-terminal α1 helix of VEGF-B (VGB1) and evaluated the possibility of its interaction with both VEGFR-1 and VEGFR-2 by *in silico* studies. The molecular modeling and CD spectroscopy studies suggested the probability of an α helix secondary structure in the peptide. Given the important role of the N-terminal α1 helix in the interaction of both VEGF-B and VEGF-A with their receptors, the possibility of the presence of this secondary structure will increase the peptide opportunity to compete with these molecules. The results from molecular docking studies showed that VGB1, like the corresponding fragment from VEGF-B, bound to the receptor mainly by hydrophobic

interactions and theoretically should capable in competing with the VEGF-B to bind with VEGFR-1. These results also proposed that probably VGB1 is capable in binding to VEGFR-2 and both hydrophobic and electrostatic interactions contribute to receptor-ligand binding. From the theoretical perspective, this peptide has the potential to compete with both VEGF-B and VEGF-A. Although speaking with certainty about the therapeutic potential of VGB1 requires extensive laboratory studies, we believe that this study will be useful toward inhibiting tumor growth and metastasis.

Author's contribution

S.M.A. directed this work. S.M.A. and E.A. performed peptide design. S.M.A., E.A. and F.M performed analysis and interpretation of data. S.M.A. and F.M supported administration of the present study. S.M.A., E.A. and F.M. wrote the present paper and have given approval to the final version of the manuscript.

Acknowledgment

The support of the University of Guilan is gratefully acknowledged.

Conflict of interest

The authors declare that there is no conflict of interest associated with this study.

References

1. Folkman J, editor. Angiogenesis and apoptosis. *Semin. Cancer Biol.* Elsevier. 2003.
2. Iyer S, Acharya KR. Tying the knot: The cystine signature and molecular-recognition processes of the vascular endothelial growth factor family of angiogenic cytokines. *FEBS J.* 2011;**278**(22):4304-4322. doi:10.1111/j.1742-4658.2011.08350.x
3. Ferrara N, Kerbel RS. Angiogenesis as a therapeutic target. *Nature*. 2005;**438**(7070):967.
4. Shibuya M. Vascular endothelial growth factor (VEGF) and its receptor (VEGFR) signaling in angiogenesis: a crucial target for anti-and pro-angiogenic therapies. *Genes Cancer*. 2011;**2**(12):1097-1105. doi:10.1177/1947601911423031
5. Guo S, Colbert LS, Fuller M, Zhang Y, Gonzalez-Perez RR. Vascular endothelial growth factor receptor-2 in breast cancer. *Biochim Biophys Acta Rev Cancer*. 2010;**1806**(1):108-121. doi:10.1016/j.bbcan.2010.04.004.
6. Rahimi N. VEGFR-1 and VEGFR-2: two non-identical twins with a unique physiognomy. *Front Biosci*. 2006;**11**:818. doi:10.2741/1839
7. Nishida N, Yano H, Nishida T, Kamura T, Kojiro M. Angiogenesis in cancer. *Vasc Health Risk Manag*. 2006;**2**(3):213-219.
8. Olofsson B, Pajusola K, Kaipainen A, Von Euler G, Joukov V, Saksela O, *et al.* Vascular endothelial growth factor B, a novel growth factor for endothelial cells. *Proc Natl Acad Sci U S A*. 1996;**93**(6):2576-2581. doi:10.1073/pnas.93.6.2576
9. Paavonen K, Horelli-Kuitunen N, Chilov D, Kukk E, Pennanen S, Kallioniemi O-P, *et al.* Novel human vascular endothelial growth factor genes VEGF-B and VEGF-C localize to chromosomes 11q13 and 4q34, respectively. *Circulation*.1996;**93**(6):1079-1082. doi:10.1161/01.cir.93.6.1079
10. Li X, Lee C, Tang Z, Zhang F, Arjunan P, Li Y, *et al.* VEGF-B: a survival, or an angiogenic factor? *CELL ADHES MIGR*. 2009;**3**(4):322-327.
11. Wiesmann C, Fuh G, Christinger HW, Eigenbrot C, Wells JA, de Vos AM. Crystal structure at 1.7 Å resolution of VEGF in complex with domain 2 of the Flt-1 receptor. *Cell*. 1997;**91**(5):695-704. doi:10.1016/s0092-8674(00)80456-0
12. Muller YA, Christinger HW, Keyt BA, de Vos AM. The crystal structure of vascular endothelial growth factor (VEGF) refined to 1.93 Å resolution: multiple copy flexibility and receptor binding. *Structure*. 1997;**5**(10):1325-1338. doi:10.1016/s0969-2126(97)00284-0
13. Iyer S, Darley PI, Acharya KR. Structural Insights into the Binding of Vascular Endothelial Growth Factor-B by VEGFR-1D2 Recognition and Specificity. *J Biol Chem*. 2010;**285**(31):23779-23789. doi:10.1074/jbc.m110.130658
14. Eswar N, Webb B, Marti-Renom MA, Madhusudhan M, Eramian D, Shen My, *et al.* Comparative protein structure modeling using Modeller. *Curr Protoc Bioinformatics*. 2006;**15**(1):5.6. 1-5.6. 30. doi:10.1002/0471250953.bi0506s15
15. Abraham MJ, Murtola T, Schulz R, Páll S, Smith JC, Hess B, *et al.* GROMACS: High performance molecular simulations through multi-level parallelism from laptops to supercomputers. *SoftwareX*. 2015;**1**:19-25. doi:10.1016/j.softx.2015.06.001
16. Schmid N, Eichenberger AP, Choutko A, Riniker S, Winger M, Mark AE, *et al.* Definition and testing of the GROMOS force-field versions 54A7 and 54B7. *Eur. Biophys. J*. 2011;**40**(7):843. doi:10.1007/s00249-011-0700-9
17. Tao Y, Rao Z-H, Liu S-Q. Insight derived from molecular dynamics simulation into substrate-induced changes in protein motions of proteinase K. *J Biomol Struct Dyn*. 2010;**28**(2):143-157.
18. Zhang Y, Skolnick JJNar. TM-align: a protein structure alignment algorithm based on the TM-score. *Nucleic Acids Res*. 2005;**33**(7):2302-2309. doi:10.1093/nar/gki524
19. Van Zundert G, Rodrigues J, Trellet M, Schmitz C, Kastritis P, Karaca E, *et al.* The HADDOCK2. 2 web server: user-friendly integrative modeling of biomolecular complexes. *J Mol Biol*. 2016;**428**(4):720-725. doi:10.1016/j.jmb.2015.09.014
20. Ellman GL. A colorimetric method for determining low concentrations of mercaptans. *Arch Biochem Biophys*. 1958;**74**(2):443-450.
21. Ellman GL. Tissue sulfhydryl groups. *Arch Biochem Biophys*. 1959;**82**(1):70-77.
22. García-Aranda MI, González-López S, Santiveri CM, Gagey-Eilstein N, Reille-Seroussi M, Martín-Martínez M, *et al.* Helical peptides from VEGF and Vammin hotspots for modulating the VEGF–VEGFR interaction. *Org Biomol Chem*. 2013;**11**(11):1896-1905. doi:10.1039/c3ob27312a
23. Wang L, Zhou L, Reille-Seroussi M, Gagey-Eilstein N, Broussy S, Zhang T, *et al.* Identification of peptidic antagonists of vascular endothelial growth factor receptor 1 by scanning the binding epitopes of its ligands. *J Med Chem*. 2017;**60**(15):6598-6606. doi:10.1021/acs.jmedchem.7b00283
24. Wang L, Gagey-Eilstein N, Broussy S, Reille-Seroussi M, Huguenot F, Vidal M, *et al.* Design and synthesis of C-terminal modified cyclic peptides as VEGFR1 antagonists. *Molecules*.

2014;**19**(10):15391-15407. doi:10.3390/molecules191015391
25. Benkert P, Tosatto SC, Schomburg D. QMEAN: A comprehensive scoring function for model quality assessment. *Proteins*. 2008;**71**(1):261-277. doi:10.1002/prot.21715
26. Miller III BR, McGee Jr TD, Swails JM, Homeyer N, Gohlke H, Roitberg AE. MMPBSA. py: an efficient program for end-state free energy calculations. *J. Chem. Theory Comput*. 2012;**8**(9):3314-3321.
27. D'Andrea LD, Iaccarino G, Fattorusso R, Sorriento D, Carannante C, Capasso D, *et al.* Targeting angiogenesis: structural characterization and biological properties of a de novo engineered VEGF mimicking peptide. *Proc Natl Acad Sci*. 2005;**102**(40):14215-14220. doi:10.1073/pnas.0505047102
28. Giordano RJ, Cardó-Vila M, Lahdenranta J, Pasqualini R, Arap W. Biopanning and rapid analysis of selective interactive ligands. *Nat Med*. 2001;**7**(11):1249. doi:10.1038/nm1101-1249
29. Giordano RJ, Anobom CD, Cardó-Vila M, Kalil J, Valente AP, Pasqualini R, *et al.* Structural basis for the interaction of a vascular endothelial growth factor mimic peptide motif and its corresponding receptors. *Chem Biol*. 2005;**12**(10):1075-1083. doi:10.1016/j.chembiol.2005.07.008
30. Giordano RJ, Cardó-Vila M, Salameh A, Anobom CD, Zeitlin BD, Hawke DH, *et al.* From combinatorial peptide selection to drug prototype (I): targeting the vascular endothelial growth factor receptor pathway. *Proc Natl Acad Sci*. 2010;**107**(11):5112-5117. doi:10.1073/pnas.0915141107